



Universiteit  
Leiden  
The Netherlands

## **The Montgomery Thyroplasty Implant System: A 360° Assessment**

Desuter, G.R.R.

### **Citation**

Desuter, G. R. R. (2020, January 21). *The Montgomery Thyroplasty Implant System: A 360° Assessment*. Retrieved from <https://hdl.handle.net/1887/83254>

Version: Publisher's Version

License: [Licence agreement concerning inclusion of doctoral thesis in the Institutional Repository of the University of Leiden](#)

Downloaded from: <https://hdl.handle.net/1887/83254>

**Note:** To cite this publication please use the final published version (if applicable).

Cover Page



Universiteit Leiden



The handle <http://hdl.handle.net/1887/83254> holds various files of this Leiden University dissertation.

**Author:** Desuter, G.R.R.

**Title:** The Montgomery Thyroplasty Implant System: A 360° Assessment

**Issue Date:** 2020-01-21

## **CHAPTER 5:**

**The *Larynx Ruler* to measure height and profile of vocal folds:  
a proof of concept.**

**Abstract:**

## Introduction:

Glottic leakage during phonation is a direct consequence of unilateral vocal fold paralysis. This air leakage can be in the horizontal plane as well as in the vertical plane. Presently there is no easily applicable medical device allowing noninvasive, office-based measurement of the relative vertical position of the vocal folds. The Larynx Ruler (LR) is a laser-based measuring device that could meet the previously stated need, using a flexible endoscope. This study represents a proof of concept regarding the use of the LR in assessing vocal fold relative positions in the vertical plane.

## Material and methods:

One fresh male human cadaver larynx, free of neurologic and anatomic disease, was explored with the LR system through the operative channel of a flexible gastroenterology video-endoscope. The tip of the video-endoscope was located in the laryngeal vestibule. The right crico-arytenoid joint was posteriorly disarticulated. Tilting of the vocal fold (VF) was obtained by pulling or pushing the arytenoid cartilage with a mosquito forceps fixed to the stump of the previously sectioned superior tip of the posterior crico-arytenoid muscle allowing anterior and posterior tilting of the arytenoid cartilage in order to induce an elevation or a depression of the VF process. Ten “push” and ten “pull” sessions were performed. The distance from the tip of the video-endoscope to each illuminated pixel of the laser beam was recorded. The level difference between the left and right VF’s was measured for each recording.

## Results:

Data provided by the LR were consistently in accordance with the movements applied on the vocal folds. The accuracy of 0.2 mm of the LR is compatible with the envisioned applications for the human larynx.

## Conclusions:

The LR system represents a feasible technique to evaluate respective vertical position of vocal folds in the human larynx. Technical limitations were identified that will require improvements before experimental use on human.

**Level of Evidence: NA**

**Key words: laryngoscopy, laser, measurement device, unilateral vocal fold paralysis**

## **Introduction**

During phonation, the closed vocal folds (VF) offer resistance to the air expelled by the lungs during expiration. Their vibro-elastic properties allow to interrupt the air flow that eventually will lead to vibration of the vocal folds and creation of sound.

The VF are located in the midpart of the thyroid cartilage. Their common anterior insertion is fixed at the anterior commissure. Their posterior anchoring corresponds to the vocal process of each arytenoid cartilage and is mobile in the three dimensions. The position of the vocal process is determined by the balanced contraction of all intrinsic laryngeal muscles under the neurological control of the vagal nerve and its terminal branches. Under normal conditions, the position of both vocal processes will be located at equal distance from any reference point located at the midline of the larynx.

In case of innervation unbalance of the larynx, for example in unilateral vocal fold paralysis (UVFP) the above-mentioned symmetry will be disrupted and may result in incomplete glottic closure during phonation leading to leakage of air at the level of the glottis. This innervation unbalance of the larynx will not only lead to a closure defect in the horizontal or axial plane but possibly also, in the vertical or coronal plane. This is why determination of the exact three-dimensional position of the posterior part of the VF is key when it comes to pre-operative planning of UVFP treatment.

As a matter of fact, the best treatment strategy to obtain optimal voice outcome after UVFP treatment is still debated. Most discussions concentrate on addressing posterior leakage. For instance, some authors advocate a systematic arytenoid adduction strategy, while others deny any use to it at all (1-6). The truth is that no evidence exists and the question remains unanswered (7-8).

Determination of the VF exact three-dimensional position before and after treatment could help to answer the above-mentioned question. Three-dimensional CT imaging has shown its value in tackling this problem but requires patient irradiation and delayed image processing. Presently there is no device allowing, real-time, harm free and office-based quantification of vocal fold vertical relative position. Industry is developing 3D video-endoscopic imaging but quantification of exact VF position remains impossible.

The Larynx Ruler (LR) is a laser based, endoscopically guided, measuring device that could meet the previously stated needs.

The primary purpose of this study is to see whether the LR technology could measure relative VF height (or level) differences, between the right and the left VF, measured from the tip of the endoscope.

## Material and methods

### The Laryngeal Ruler (LR) Device.

The LR device consists of a laser probe based on a miniaturized pattern projector placed in the instrument channel of the endoscope (Olympus GIF-100, Hamburg, Germany). It has a diameter of 2.7mm (Figure 1) and projects a line used as reference for analysis.

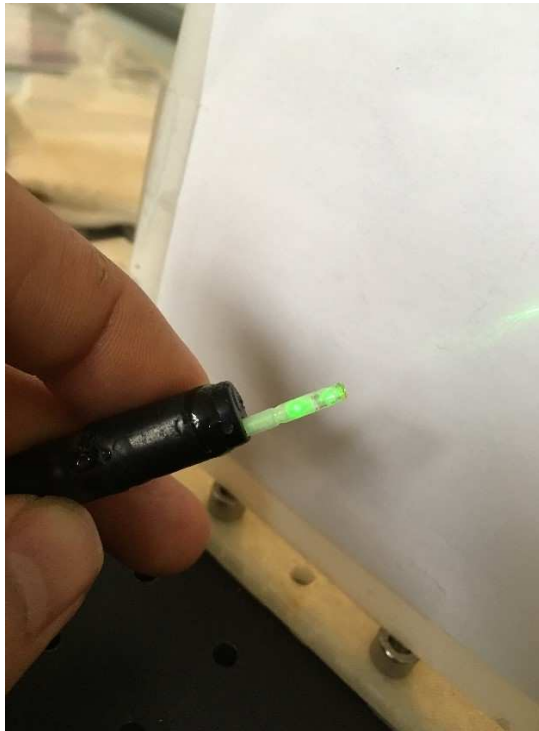


**Figure 1:** Laser probe placed in the instrument channel of the endoscope.

Principle of 3D reconstruction:

The LR is based on the structured light technology. A known pattern is projected and its image is analyzed to recover the 3D position of the points of interest (Figure 2). The projector  $P$  projects a laser line towards a point  $A$  on a surface, the camera  $C$  acquires the image. Depth ( $z$ ) is then easily calculated as,  $\alpha$  is the angle of projection measured using the pixel position of the point  $A$  as detailed in ,  $\beta$  is known by calibration.9.It is the angle of projection of the line in the camera coordinates, and the distance  $d$  (between camera and projector) is the baseline known by calibration. 10.It can be easily shown that:

$$z = \frac{d}{\tan(\alpha) - \tan(\beta)}$$

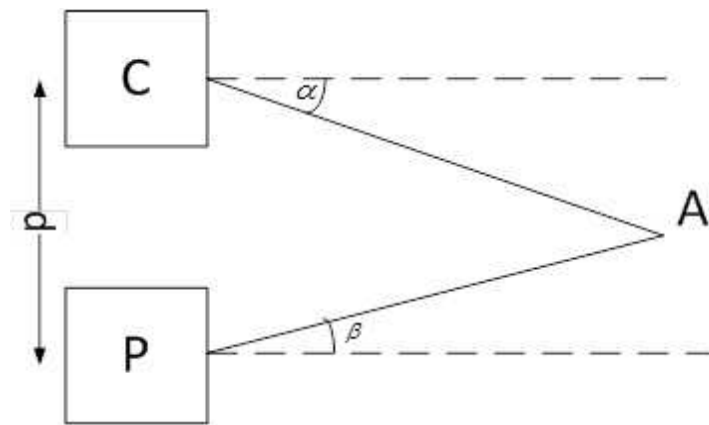


**Figure 2:** The point  $A$  is found by triangulation knowing the baseline  $d$  and the angles  $\alpha$  and  $\beta$ .

In this example, the system is brought back to a 2D system, but it can be generalized to a 3D system. More information about structured light 3D reconstruction can be found in. 9.

Projection principle:

The projection is based on a diffracted laser beam using a diffractive optical element (DOE). DOE's are commercially available (e.g. Holoeye, Berlin, Germany) and are engraved to project a pattern (in this case, a simple line) as a focused laser beam pass through it (Figure 3). The pattern used is a single line, placed perpendicularly to the epipolar plane. It enables a direct measurement of every point of the line.

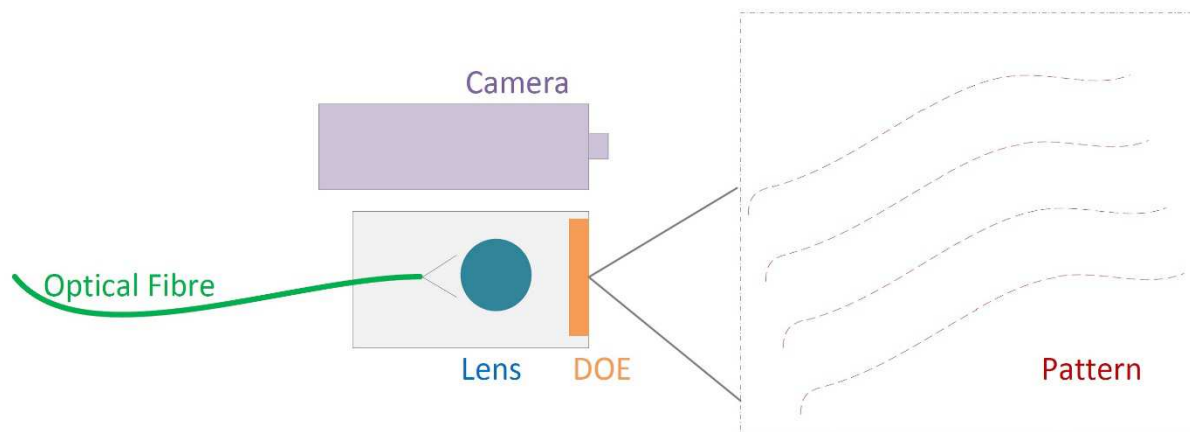


**Figure 3:** The system is composed of an optical fiber to transmit the beam, a lens to focus it and a diffractive optical element (DOE) to generate the pattern. The pattern is then analyzed using the camera of the endoscope.

This principle was already used by several authors have both developed a device based on two laser dots that provide a mean for estimating depth of the region of interest. 11.12.13. However, in this solution, the measurements are based on approximations. If the region of interest is not flat, it could lead to relatively important errors. Neitsch et al have proposed a smart solution based on a matrix of points (instead of two points).14. The main limitation here is that measurements are possible only where points are projected (or detectable). The laser source has a maximum power of 20mW at a wavelength of 532nm.

With regard to safety, the power density is lower than a conference laser pointer as the beam is used for a complete line whereas a laser pointer is focused on a single point. The power density is of  $16 \text{ W/m}^2$  with a total power lower than 1mW. LR is thus harm-free for the patient.

The accuracy of this technology has been demonstrated elsewhere (9).

In a nutshell, the accuracy can be calculated by:

$$\delta z = \frac{\delta p_x z^2}{d f_x}$$

Where:

- $\delta z$  is the accuracy (in m);
- $\delta p_x$  is the accuracy of the line detection (in pixel);
- $z$  is the working depth (in m);
- $d$  is the baseline (distance between the camera and the projector, in m);
- $f_x$  is the focal length of the camera (in pixels) .

### Measuring process

The probe is kept in place by friction, the diameter of the device being the same as the channel diameter. The user places the device in the instrument channel and calibrates it before performing the endoscopy. The user checks the calibration (a ruler is used as reference) before and after performing the endoscopy.

To proceed with the measurement, the following steps were followed:

1. The endoscopist places the endoscope in a way the line is placed where the measurement must be made. The image is then freeze.
2. An external dedicated computer acquires the image and processes it to compute the data.
3. The user may picks-up the points of interest for exact measurements.
4. Data is displayed instantaneously on the endoscopic image and the profile in a dedicated window.

Homemade dedicated software using the Open CV library is used to compute the complete profile based on the equations mentioned here above. The system is calibrated prior any use to take the lens distortion and the tolerances of assembly into account. The processing time is below 50ms.

The generated profile is required to provide the user the ability to select exactly the relevant points of interests. In addition to that, the points of interests are shown on both the endoscopic image and the 3D profile to make sure the distances are relevant. Therefore, the user is able to select visually the points of interest by considering the anatomical structures on the endoscopic image itself.

However, the position of the tip of the endoscope (specially a possible angle-view) related to the larynx must be understood by the user to properly understand the generated profiles. The distance of the endoscope to the larynx has no influence as the profile is generated in 3D (it simply moves the profile along depth).

Height measurements at each pixel points of the laser-illuminated structures open the field of three-dimensional assessment of the larynx.

#### Proof of concept measurements

The study protocol was approved by the University of Louvain Institutional Ethical Committee under the number 2017/18JAN/028. The anatomical material was harvested according to Institutional Ethical Committee regulations.

One fresh unfrozen human male larynx was used for assessment of VF heights. According to patient medical file examination and anatomical inspection, the larynx was declared free of disease.

The specimen was examined with the LR system through the operative channel of a gastroenterology video-endoscope (Olympus GIF-100, Hamburg, Germany). The tip of the video-endoscope was positioned in the laryngeal vestibule. Experimental setting is detailed in Figure 4.

The right crico-arytenoid joint of the larynx was posteriorly disarticulated allowing anterior and posterior tilting of the arytenoid cartilage in order to create an elevation or a depression of the VF process. Tilting of the VF was obtained by pulling or pushing the arytenoid cartilage with a mosquito forceps fixed to the stump of the previously sectioned superior tip of the posterior crico-arytenoid muscle. The experimentally induced “push-and-pull” motions were compared at a given time with VF distances measured from the tip of the endoscope provided the LR technology. Ten “push” and ten “pull” sessions were performed. The distance from the tip of the video-endoscope to each illuminated pixel of the laser beam was recorded and plotted on a diagram (Figure 5). The level difference between the left and right VF’s was measured for each recording.

A vocal fold profile, showing the surface of the laser illuminated VF, was realized during each measurement. Profile characteristics that were scrutinized were: (a) ease of finding the medial edge pixel of VFs; (b) seamless surface profile of the VF and (c) identification of Morgani’s ventricles gap.

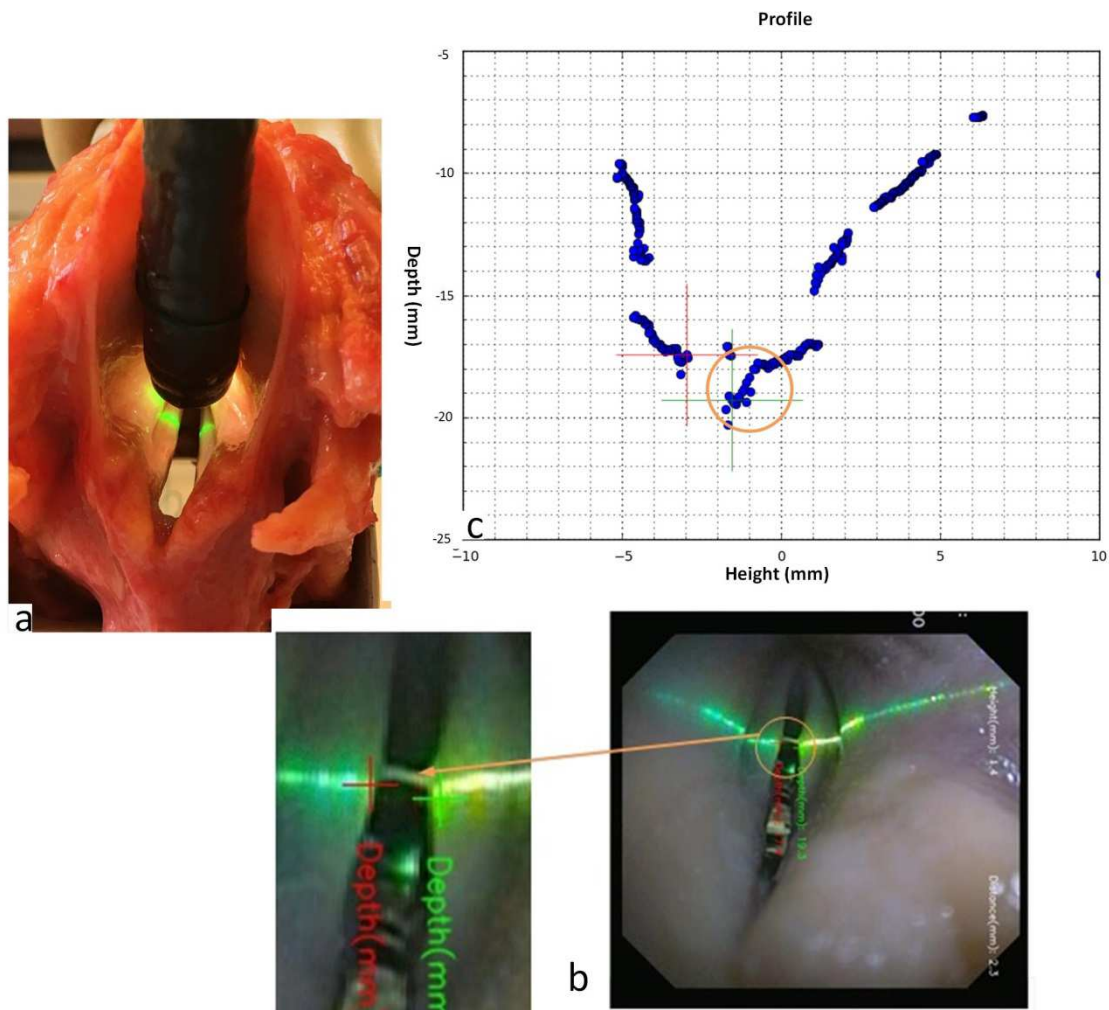


**Figure 4:** (a) Study setting showing the operative video-gastroscope introduced into the larynx vestibule with the laser beam “scanning” both vocal folds. (b) Endoscopic image of the laser beam “scanning” the glottis and the larynx vestibule; a zoomed image shows the respective positions of VF medial edges where VF height was measured from the tip of the video-endoscope (crosses represent medial free edges (green=right, red=left); note the fortuitous presence of a secretion between the vocal folds at the level of the laser beam) (c) LR screen capture showing the section profile by plotting heights measured from the tip of the video-endoscope, of every pixel that is illuminated along the laser beam.

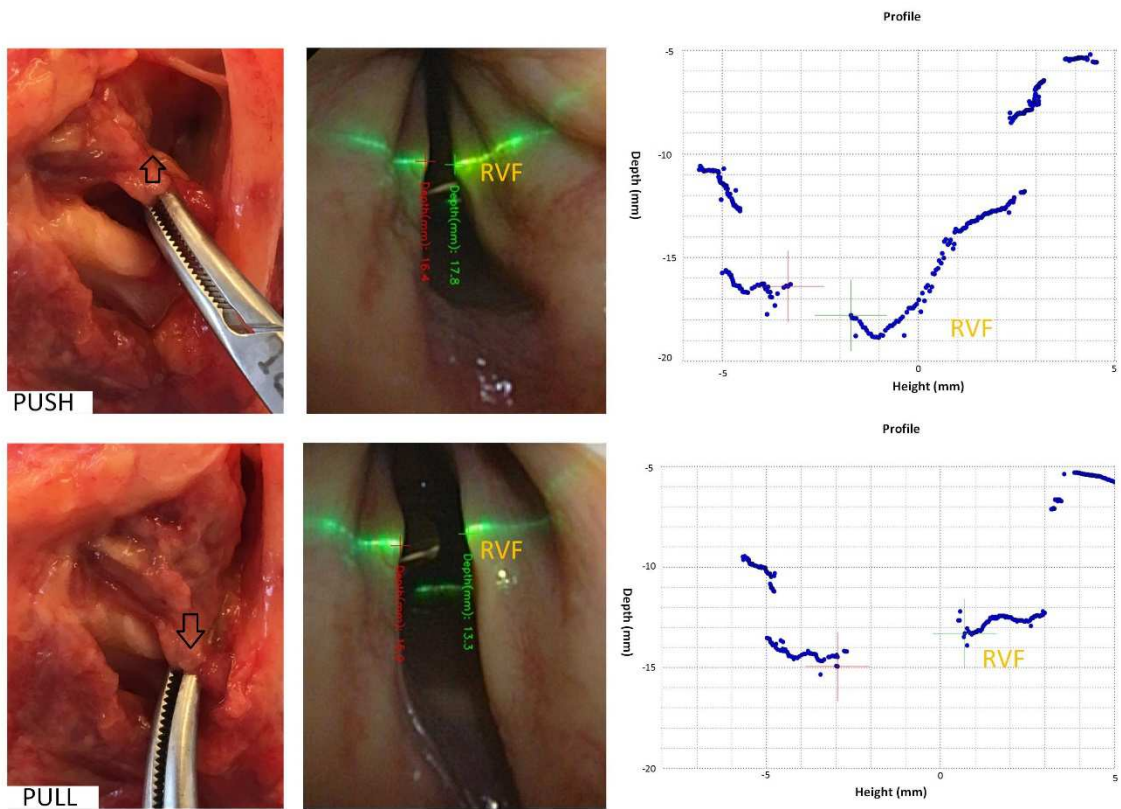


**Figure 5:** shows from left to right; simultaneous images of (1) The arytenoid motion applied on the specimen by a mosquito forceps on the posterior crico-arytenoid muscle stump. The *push motion* opens the crico-arytenoid joint and glides the arytenoid cartilage down internally on the cricoid cartilage. This lowers the VF. The *pull motion* glides the arytenoid posteriorly on the cricoid crest. This elevates the VF (2) The endoscopic image obtained with the LR video-endoscope showing the laser beam position (3) the corresponding screen capture provided by the LR. Note the difference of heights between VFs visualized and quantified on the screen capture images. These differences are not clearly visible on 2D endoscopic images.

## Result

The results are shown in table 1. There was a perfect correlation between the relative position of the VFs (above or below the contralateral control side) and the relative heights measured by the LR technology. In other words, using the LR, it was possible to detect and quantify the difference in VF heights, measured from the tip of the video-endoscope, induced by manipulating the arytenoid cartilage. The force applied on the arytenoid cartilage was different for each session; therefore, the value of the height difference was variable. Likewise, the position of the tip of the endoscope was not completely fixed thus the absolute value of the VF height was different for each measurement.

Sessions	PUSH of the Right Arytenoid			PULL of the Right Arytenoid		
	Left VF height (mm)	Right VF height (mm)	Relative position of mobilized (right) VF (mm)	Left VF height (mm)	Right VF height (mm)	Relative position of mobilized (right) VF (mm)
1	17.6	19.5	1.9 mm Below	14.8	12.7	2.1 mm Above
2	14.5	16.2	1.7 mm Below	14.2	12.9	1.3 mm Above
3	15.9	16.8	0.9 mm Below	15.9	12.8	3.1 mm Above
4	18.6	21.7	3.1 mm Below	12.4	10.4	2.0 mm Above
5	20.0	22.5	2.5 mm Below	19.1	16.5	2.6 mm Above
6	18.4	20.2	1.8 mm Below	16.7	14.8	1.9 mm Above
7	16.4	17.8	1.4 mm Below	15.0	13.3	1.7 mm Above
8	19.6	21.4	1.8 mm Below	16.8	14.0	2.8 mm Above
9	11.3	16.5	5.2 mm Below	13.6	12.2	1.4 mm Above
10	15.0	17.9	2.9 mm Below	15.0	13.2	1.8 mm Above

**Table 1:** Table indicating, for each session, VF heights from the tip of the video-endoscope and the relative position of the mobilized VF.

The profiles were measured during the endoscopy and were available for post checking after the endoscopy.

A profile (or shape) of the surface of the VF at the level of the LR laser beam was always obtainable. This profile offers a visualization of a virtual coronal section of the VF at the level of LR's laser beam (Figure 6).

VF heights could be measured in all the evaluated positions. In 4 of the 20 screen captures, a seamless profile was not obtainable. These profiles were discontinuous and did not allow a clear profiling of glottic surface. Despite these caveats, Morgani's ventricles depths were always visible and quantifiable. No tissue damage was observed.

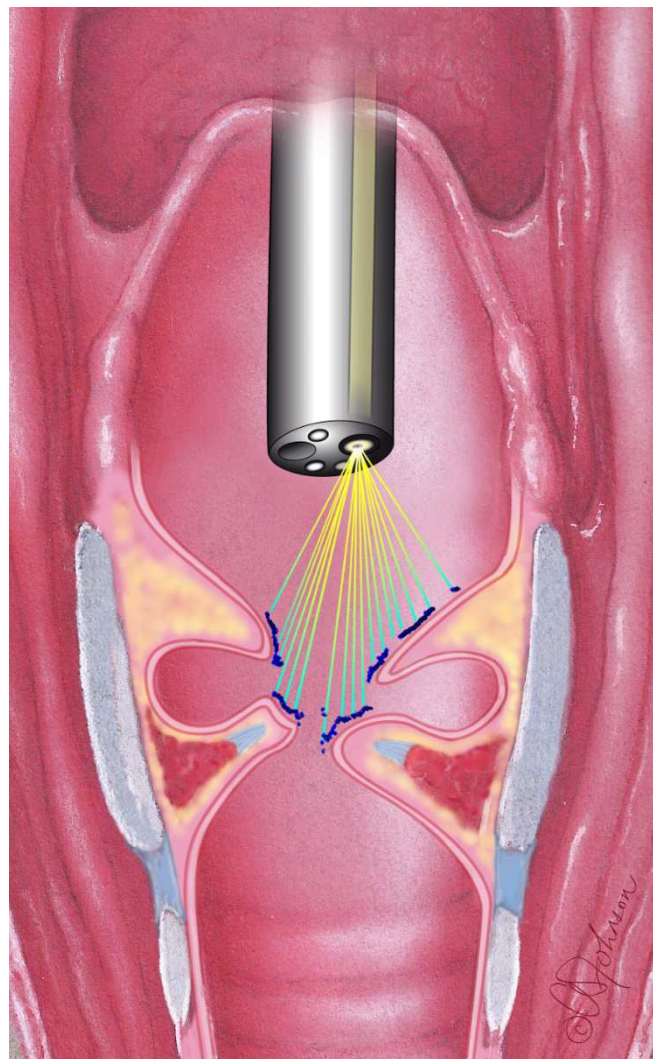


**Figure 6:** Drawing figuring the relationship between the scanning laser beam and the “profile” offered by the LR data interpretations

## Discussion:

Our results show that use of the LR is technically feasible in a human larynx. A perfect correlation of VF height differences between left and right vocal folds and imposed VF motions was found. Qualitative analysis showed that a VF profile was obtainable in all of the push-pull sessions. The aim of this *proof-of-concept* was not to assess the accuracy of the LR but rather to assess its possible utility in the laryngology field in general and in UVFP management in particular.

Nevertheless, in the case of our experiment in the larynx, with a distance between the LR and the VF of approximately 2 cm, the accuracy is about 0.2 mm which is compatible with the foreseen clinical applications of LR. Indeed, none of our height differences were less than 0.9 mm.

At present, there is considerable interest concerning the topic of three-dimensional positioning of the vocal fold for which MRI and CT studies in patients have been performed as well as laryngoscopic high-speed camera imaging in animal models 15. MRI has a lower resolution and CT scanner necessitates radiation exposure and post-acquisition software based interpretation 16.17.18.19.20. Both these imaging techniques are costly and do not allow for the examination of patients under physiological conditions. The high-speed camera does not have the disadvantage of irradiation but requires two simultaneously introduced endoscopes and 2 high-speed cameras. Furthermore, it also requires post-recording analysis, so it does not yield real-time readings. Compared to prior articles using the same technology, apart from application using a flexible endoscope, it is the first experiment with a continuous line and it enables a fine analysis of the vocal fold with the generated profile. 11.12.13.14.

Profiling of the explored surfaces can be realized using multiplication of the acquired measures. As shown in Figure 6, profiling of VF surface could possibly reflect and quantify the degree of TA atrophy in cases of UVFP. Some of these profiles were discontinuous and tedious to read. Technical refinements and adaptations that are specific to the larynx anatomy should be done in order to offer clinically useful profiles.

Despite these encouraging results many challenges still have to be overcome before the LR use in patients. The endoscope that was used is a gastroscope (11mm of diameter) which is too large for intranasal use. A device with a maximum diameter of 1.9 mm should be developed to allow its use through the operative channel of ENT flexible video-endoscope. Specific software for vocal fold analysis and interpretation should be developed to improve the profile representations and height measurement in a more reliable way.

In our study models, the vocal processes were always easily visualized. However, in clinical UVFP situations, the vocal process on the paralyzed side, can be difficult to

visualize due to the anterior tilt of the arytenoid cartilage. Hypothetically, this hurdle could be overcome by the development of software that would (a) measure various VF free edge points that can be effectively visualized, (b) draw a line through these points, (c) calculate the VF free edge slope, and eventually (d) extrapolate the invisible VF depth based on the contralateral VF length.

## **Conclusion**

Innovative technology is not so frequent in the field of laryngology. This *proof of concept* could signify a new breakthrough. Study's results allow authors to achieve their goal of demonstrating potential utility of the device. With the LR technology, a tool is acquired that allows a reliable, real-time, three-dimensional position determination of the vocal folds, free of harm for the patient and instantaneously performed within an office setting. Therefore, it contributes to pre-operative planning of laryngeal surgery as well as the post-operative follow-up. The LR technology deserves further clinical testing, even though several technical improvements are still required.

## References

1. Daniero JJ, Garrett CG, Francis DO. Framework Surgery for Treatment of Unilateral Vocal Fold Paralysis. *Curr Otorhinolaryngol Rep.* 2014 Jun;2(2):119-130. PubMed PMID: 24883239; PubMed Central PMCID: PMC4036824.
2. Hess MM, Fleischer S. Laryngeal framework surgery: current strategies. *Curr Opin Otolaryngol Head Neck Surg.* 2016 Dec;24(6):505-509. PubMed PMID: 27585082.
3. Li AJ, Johns MM, Jackson-Menaldi C, Dailey S, Heman-Ackah Y, Merati A, Rubin AD. Glottic closure patterns: type I thyroplasty versus type I thyroplasty with arytenoid adduction. *J Voice.* 2011 May;25(3):259-64. doi:10.1016/j.jvoice.2009.11.001. PubMed PMID: 20335002.
4. Mortensen M, Carroll L, Woo P. Arytenoid adduction with medialization laryngoplasty versus injection or medialization laryngoplasty: the role of the arytenoidopexy. *Laryngoscope.* 2009 Apr;119(4):827-31. doi: 10.1002/lary.20171. PubMed PMID: 19263407.
5. Woo P. Arytenoid adduction and medialization laryngoplasty. *Otolaryngol Clin North Am.* 2000 Aug;33(4):817-40. PubMed PMID: 10918663.
6. Benninger MS, Manzoor N, Ruda JM. Short- and long-term outcomes after silastic medialization laryngoplasty: are arytenoid procedures needed? *J Voice.* 2015 Mar;29(2):236-40. doi: 10.1016/j.jvoice.2014.07.008. PubMed PMID: 25510165.
7. Siu J, Tam S, Fung K. A comparison of outcomes in interventions for unilateral vocal fold paralysis: A systematic review. *Laryngoscope.* 2016 Jul;126(7):1616-24. doi:10.1002/lary.25739. Review. PubMed PMID: 26485674.
8. Chester MW, Stewart MG. Arytenoid adduction combined with medialization thyroplasty: an evidence-based review. *Otolaryngol Head Neck Surg.* 2003 Oct;129(4):305-10. Review. PubMed PMID: 14574281.
9. Mertens, B., & Delchambre, A. (2016). 3D reconstruction: Why should the accuracy always be presented in the pixel unit? *Image and Vision Computing, 48*, 57-60.
10. Geng, J., 2011. Structured-light 3d surface imaging: A tutorial. *Advances in Optics and Photonics 3* (2), 128-160.11.
11. Herzon GD, Zelear DL. New laser ruler instrument for making measurements through an endoscope. *Otolaryngol Head Neck Surg.* 1997 Jun;116(6 Pt 1):689-92. PubMed PMID: 9215386.

12. Kuo CF, Wang HW, Hsiao SW et al. (2014) Development of laryngeal video stroboscope with laser marking module for dynamic glottis measurement. *Comput Med Imaging Graph* 38:34-41
13. Schade G, Hess M, Rassow B. [Possibility for endolaryngeal morphometric measurements with a new laser light method]. *HNO*. 2002 Aug;50(8):753-5. German.
14. Neitsch M, Horn IS, Hofer M, Dietz A, Fischer M. Integrated Multipoint-Laser Endoscopic Airway Measurements by Transoral Approach. *Biomed Res Int*. 2016;2016:6838697. doi: 10.1155/2016/6838697. Epub 2016 Feb 15.
15. Vahabzadeh-Hagh AM, Zhang Z, Chhetri DK. Quantitative Evaluation of the In Vivo Vocal Fold Medial Surface Shape. *J Voice*. 2017 Jan 12. pii S0892-1997(16)30320-4. doi: 10.1016/j.jvoice.2016.12.004. [Epub ahead of print. PubMed PMID: 28089390.
16. Vachha BA, Ginat DT, Mallur P, Cunnane M, Moonis G. "Finding a Voice": Imaging Features after Phonosurgical Procedures for Vocal Fold Paralysis. *AJNR Am J Neuroradiol*. 2016 Sep;37(9):1574-80. doi: 10.3174/ajnr.A4781. Review.
17. Burdumy M, Traser L, Burk F, Richter B, Echternach M, Korvink JG, Hennig J, Zaitsev M. One-second MRI of a three-dimensional vocal tract to measure dynamic articulator modifications. *J Magn Reson Imaging*. 2016 Dec 9. doi:10.1002/jmri.25561. [Epub ahead of print] PubMed PMID: 27943448
18. Vorik A, Unteregger F, Zwicky S, Schiwowa J, Potthast S, Storck C. Three-dimensional Imaging of High-resolution Computer Tomography of Singers' Larynges-A Pilot Study. *J Voice*. 2016 Jul 11. pii: S0892-1997(16)30044-3. doi:10.1016/j.jvoice.2016.03.011. [Epub ahead of print] PubMed PMID: 27427164.
19. Storck C, Juergens P, Fischer C, Wolfensberger M, Honegger F, Sorantin E, Friedrich G, Gugatschka M. Biomechanics of the cricoarytenoid joint: three-dimensional imaging and vector analysis. *J Voice*. 2011 Jul;25(4):406-10. doi: 10.1016/j.jvoice.2010.03.005. PubMed PMID: 20579841.
20. Hiramatsu H, Tokashiki R, Kitamura M, Motohashi R, Tsukahara K, Suzuki M. New approach to diagnose arytenoid dislocation and subluxation using three-dimensional computed tomography. *Eur Arch Otorhinolaryngol*. 2010 Dec;267(12):1893-903. doi: 10.1007/s00405-010-1300-5. PubMed PMID: 20549225.

## **Acknowledgments**

Authors are thankful to C. Behets-Wydemans, B. Caelen and M. van de Woestijne from the department of Anatomy and Morphology of the University of Louvain and F. van Immerseel, J Aarents and J. den Boeft from the department of Anatomy and Embryology at the Leiden University Medical Center for their assistance.